

The Friction of Structurally Modified Isotactic Polypropylene

Natalia Wierzbicka ^{1,*} , Tomasz Sterzyński ¹  and Marek Nowicki ² 

¹ Faculty of Mechanical Engineering, Poznan University of Technology, Piotrowo 3, 60-965 Poznan, Poland; Tomasz.Sterzynski@put.poznan.pl

² Faculty of Materials Engineering and Technical Physics, Poznan University of Technology, Piotrowo 3, 60-965 Poznan, Poland; marek.nowicki@put.poznan.pl

* Correspondence: natalia.wierzbicka@put.poznan.pl

Abstract: The purpose of studies was to analyse an impact of heterogeneous nucleation of modified isotactic polypropylene (iPP) on its tribological properties. The iPP injection molded samples, produced by mold temperature of 20 and 70 °C, were modified with compositions of two nucleating agents (NA's), DMBDS creating α -form and mixture of pimelic acid with calcium stearate (PACS) forming β -phase of iPP, with a total content 0.2 wt.% of NA's. A polymorphic character of iPP, with both, monoclinic (α) and pseudo-hexagonal (β) crystalline structures, depending on the NA's ratio, was verified. The morphology observation, DSC, hardness and tribological measurements as test in reciprocating motion with "pin on flat" method, were realized, followed by microscopic observation (confocal and SEM) of the friction patch track. It was found that Shore hardness rises along with DMBDS content, independent on mold temperature. The friction coefficient (COF) depends on NA's content and forming temperature—for upper mold temperature (70 °C), its value is higher and more divergently related to NA's composition, what is not the case by 20 °C mold temperature. The height of friction scratches and the width of patch tracks due to its plastic deformation, as detected by confocal microscopy, are related to heterogeneous nucleation modified structure of iPP.



Citation: Wierzbicka, N.; Sterzyński, T.; Nowicki, M. The Friction of Structurally Modified Isotactic Polypropylene. *Materials* **2021**, *14*, 7462. <https://doi.org/10.3390/ma14237462>

Academic Editor: Irina Hussainova

Received: 21 October 2021

Accepted: 30 November 2021

Published: 5 December 2021

Publisher's Note: MDPI stays neutral with regard to jurisdictional claims in published maps and institutional affiliations.



Copyright: © 2021 by the authors. Licensee MDPI, Basel, Switzerland. This article is an open access article distributed under the terms and conditions of the Creative Commons Attribution (CC BY) license (<https://creativecommons.org/licenses/by/4.0/>).

Keywords: isotactic polypropylene; nucleation; friction; surface analysis

1. Introduction

The polymeric materials belong now-a-days to frequently used in tribological applications. The main advantages are low friction coefficient, easy to produce even very complex sliding elements by injection molding, thus the ability to fabricate industrially applied sliding bearings used nowadays in many branches, such as sport, housekeeping, automotive, medicine etc. The sliding elements are produced mainly in large series; therefore, injection molding presents a very beneficial technique in this case.

The selection of an appropriate polymeric material, shape and dimensions of sliding elements, is a crucial feature by designing polymers for the tribological application. Before selecting the polymeric material for frictional use, the specific application conditions have to be considered.

Numerous polymers and its composites are applied currently by production of sliding elements for different industrial applications. Polymers and modified polymers, polymer blends and/or polymer composites are used now in these applications, and huge literature may be found. Various aspects of sliding are presented recently, such as studies of tribological performance for various polymers, together with role played by the counter face [1], or the results of measurements of coefficient of friction (COF) for different polymers used as slide bearings [2]. The improvement of both, tribological performance and mechanical properties are the topics of papers where the polymer matrix is modified by CNT or graphene added to polyimide [3,4] or polyethylene [5–7]. The polymeric bearings are used also in construction operating in extremely demanding conditions [8–10]. These are only few examples of recently published studies of polymers applied in tribological designing.

An important circumstance is the establishing of thermal conditions under which the frictional elements will be applied, critical case for majority of polymeric materials. The use of composites with highly resistant polymers filled with thermal conducting powders, such as carbon and/or copper, bronze, aluminum etc. metallic powder allows to overcome the problem of high temperature setting. In this case the coincidence with modification of electrical properties of such composites has to be taken into account.

Mahmoud [11] showed that the best tribological blend was composed of 25% polyethylene and 75% poly(methylmethacrylate) reinforced with bronze, leading to significant decrease in friction and wear. According to Mudradi [12] the use of recycled cast iron powder as a micro-filler for epoxy polymers resulted in reduction of specific wear rate and to decrease in the friction coefficient, compared to pure polymer.

The polymeric sliding bears are especially valuable in cases where relatively low charges are applied, and the continuous lubrication is not required. Some of the polymer-sliders may be water cooled and greased with water cooling lubrication, as it is the case of apparatus and machines working at the food industry and often at agriculture. Such designing's are also needed by construction of small housekeeping machines, where the use of self-lubricated polymeric materials allows the long utilization without external lubrication.

The relationship between an isotactic polypropylene, used without any additional fillers, however structurally modified by means of specific heterogeneous nucleation, and its tribological behaviors was the aim of our studies. Particularly, the impact of α and β iPP crystalline structure, characterized by various mechanical properties, on the deformation of the external layer of samples charged during the frictional test, was the interest of our experimental research.

Low density, relatively low price, simple processing and high modification ability, by chemical treatment, reaction of composites and by heterogonous nucleation, allowing to create desired application properties, presents main inspirations of industrial use of isotactic polypropylene and its copolymers. Another advantage is a very high popularity of this polymer, presenting pro-ecological advantages such as recycling ability with all commonly used processing techniques. These effects are described in literature, such as mechanical properties and reusability of printed circuit boards, [13] formation of materials from recycled PP blends with TPE [14] or recycled blends of polyolefins [15], use of recycled polypropylene for composites with natural fibers [16], and the reuse of industrial PP products [17]. It has to be stressed that polypropylene may easily be recycled at the end of lifetime, thus offers a limited devastation of the environment.

The early information's concerning structural modification of iPP by nucleation induced crystallization were published by Beck [18] and Binsbergen [19]; suggesting a theoretical explanation of these effect [20] based on the surface energy. Wittman and Lotz [21,22] have proposed the theory of epitaxial growth to explain the specific interaction between the nucleating agent and the crystallizing polymer.

The heterogeneous nucleation modification of the crystalline structure is a very effective and well-known method, allowing production of iPP products with desired properties. Lovinger et al. [23] presented a method of preparation of β pseudo hexagonal crystalline forms in polypropylene in temperature gradient. A huge bibliography may be found concerning the use of a small quantity of various low molecular additives as nucleating agents resulting in specific iPP crystallization (NA's) [24–29]. Two main effects may be awaited if the iPP is modified by using the NA's, the first one is characterized by an increase of the crystallization temperature T_g , allowing to shorten the processing cycles, the second one may lead to specific creation of various crystalline forms. Recently a review of known organic and nonorganic additives, playing a role of nucleation agents, was presented by Gahleitner et.al. [30].

The use of specific NA's, leading to an increase of nucleation density, thus to a morphology with small homogeneously distributed spherulites, in the crystalline polymer was published in [31–33]. Instead of creation of homo crystallization centers by local overcooling, a high number of regularly distributed NA's particles leads to formation

of heterogeneous nucleation centers, followed by its growth, which happens in a temperature higher comparing with the neat polymer. As the molten polymer begins to crystallize/solidify in higher temperature a significantly shorten cycles time is observed, an effect which is largely notable and often applied by industrial processing.

In addition to the increase of crystallization temperature, the heterogeneous nucleation leads to transformation of the crystalline structure and consequently of the properties measured even on the nano level [34–38]. This effect concerns not only the iPP homopolymer, but also its copolymers with PE [25,30,38].

A crystalline phase transition may be observed if appropriate additives are applied. The isotactic polypropylene may crystallize in three crystalline phases, i.e., in monoclinic α -phase, hexagonal β -phase and rarely in triclinic γ -phase [39–41], where the physical properties, such as mechanical strength, choc resistance, stability and even transparency are strongly the crystalline form dependent. Concerning the specific properties for the technical/industrial uses, basically only the monoclinic and hexagonal crystalline forms of iPP have found an application nowadays, because the iPP crystalized in the monoclinic form is characterized by high modulus, thus lower deformability and brittle type of break comparing with pseudo-hexagonal structure of β iPP. Another important property is an improved transparency of α -phase iPP, comparing with β -form samples, effects which schematically may be seen in Table 1.

Table 1. Mechanical properties and transparency of α -phase iPP comparing with β -form samples.

Specific Property	Monoclinic iPP α	Pseudo-hexagonal iPP β
Tensile modulus of elasticity	HIGH	LOW
Tensile elongation at break	LOW	HIGH
Impact resistance	LOW	HIGH
Optical transparency	HIGH	LOW

As mentioned before the use of low molecular additives with nucleation capacity leads to morphology with very small spherulites, even in a cylindrical form [42]. As the type and dimension of the spherulitical morphology significantly influence the polymer properties, the same nucleation density was applied in all samples, i.e., an equal quantity of NA's additives was merged into the polymeric matrix.

Our interest was to investigate polymeric samples with comparable morphology, but with various well defined crystal structures, therefore the same total quantity of 0.2 wt.% of combination of specific α and β NA's was used in all samples. Taking into account different iPP crystallization ability of both NA's, the creation of monoclinic (α) and pseudo-hexagonal (β) crystalline structures was predictable.

2. Materials and Methods

2.1. Plan of Experiments

The basic mechanical properties of an isotactic polypropylene (iPP) modified by specific heterogeneous nucleation, were evaluated as a part of this study. The surface texture and an impact of structural modification on tribological behaviors were completed as a second part of the experiments. These tests include the tribological investigations, such as determination of friction coefficient and analysis of pathway deformation.

2.2. Materials

An isotactic polypropylene Moplen HP500 N (Basell Orlen, Plock, Poland), a non-nucleated injection molding grade, without nucleating agents was used as a matrix polymer. The characteristic values of this polymer are following: MFR (210 °C, 2.16 kg) = 12 g/10 min; MFV (210 °C, 2.16 kg) = 16 cm³/10 min, density 0.90 g/cm³, HDT = 97 °C and the flexural modulus Eb = 1.48 GPa.

The 1,3:2,4- Bis (3,4-dimetylobenzylideno) sorbitol (DMDBS) Millad 3988 produced by Milliken Chemical (Gent, Belgium) was used as specific α nucleation agent, leading to creation of monoclinic crystallographic form of iPP.

According to our previous studies and to a number of publications [43–49], a 1:1 mixture of pimelic acid and calcium stearate (PACS) (both delivered by Sigma-Aldrich (Darmstadt, Germany)) in a powder form, was used as specific nucleating agent, leading to formation of the β hexagonal phase of iPP.

The composition of samples is presented in Table 2.

Table 2. Composition of iPP nucleated samples. 20 and 70 °C correspond to injection mold temperature.

Notation	Total Concentration of Additives [wt.%]	Content of NA [wt.%]	
		DMDBS	PACS
PP 20	0	-	-
DMDBS20	0.2	0.2	-
3 D1 P20	0.2	0.15	0.05
1 D1 P20	0.2	0.1	0.1
1 D3 P20	0.2	0.05	0.15
PACS20	0.2	-	0.2
PP70	0	-	-
DMDBS70	0.2	0.2	-
3 D1 P70	0.2	0.15	0.05
1 D1 P70	0.2	0.1	0.1
1 D3 P70	0.2	0.05	0.15
PACS70	0.2	-	0.2

2.3. Samples Preparation

The master batches (MB) of α and β nucleating agents, with a concentration of 0.5 wt.% each, were homogenized using a twin-screw extruder ZAMAK (Zamak Mercator, Skawina, Poland), operating at temperature 150 °C to 200 °C along the barrel, followed by solution of the MB with iPP to a concentration of 0.2 wt.%.

Regarding our primary experiments [50,51], the most suitable content is 0.2 wt.% of NA's in the iPP matrix, leading to an improvement of crystallization process and properties. On this way both, a beneficial increase of the crystallization temperature and creation of the demanded crystal phase may be achieved. Such a high content of NA's creates a stable small-spherulitical morphology of iPP, which may clearly be observed by optical microscopy [52,53]. Therefore, in our investigations the total content of nucleating agents in the polymeric matrix was fixed for all samples, equal to 0.2 wt.%.

The iPP matrix modified by α and β specific nucleating agents (DMDBS and PACS, respectively) with relative concentration of both NA's 1:0, 1:3, 1:1, 3:1 and 0:1 was examined together with neat iPP samples. Two series of nucleation modified iPP samples were investigated, produced by two injection molding with mold temperature of 20 °C and 70 °C. Due to literature and our earlier experiences, it was ascertained that even if a proper β -NA has been applied, by fast cooling at the mold, only α -phase crystals are usually achieved. This structural effect was indicated and explained by Varga [52] who found that the $T_{\alpha,\beta}$ temperature of 144 °C is critical for selective creation of both crystal phases in an isotactic polypropylene.

The samples were produced using the Battenfeld PLUS 350 (Battenfeld, Bad Oeynhausen, Germany) injection molding machine, operating by barrel temperature 210–220–220 °C, injection pressure 26 MPa, packing pressure 21.5 MPa, packing time 20/23 s and cooling time 50 s, at the dimension of 100 × 90 × 2 mm³.

2.4. Polarized Microscopic Observation

To detect the spherulitical morphology the polarized microscopic observations (POM) were realized in transmission mode. Samples in a form of slights with a thickness between

10 and 20×10^{-6} m were cut by using a Leica Microtome (Leica Microsystem, Buffalo Grove, IL, USA) on the cross section of the PP plates.

2.5. Differential Scanning Calorimetry

The differential scanning calorimetry (DSC) measurements were realized to identify the existence of both, the monoclinic and the hexagonal structure, together with the specific melting and crystallization temperature. The measurements were performed using the Netzsch DSC 204 F1 Phoenix (Netzsch, Selb, Germany) with an intercooler, operating at double heating/cooling mode, at the temperature range between 20 °C and 240 °C. The heating and cooling rate was equal to 10 °C per minutes and the average mass of samples was about 5 mg.

2.6. Wide Angle X-Ray Scattering

The X-ray diffraction analysis, with the aim to determine the type of the crystal structure of nucleation modified PP samples, was carried out by means of X-ray diffractometer Seifert FPM URD-6 (Rich Seifert-FPM, Berlin, Germany), operating by 40 kV and 20 mA, with a Bragg-Brentan geometry, at scanning angle between 10 and 40°, using the $\text{Cu}_{\text{k}\alpha}$ radiation in reflection mode. The X-ray wavelength was 0.14518 nm.

The k-value giving a quantitative information about the hexagonal β phase content was evaluated by means of Turner—Jones et al. equation in a form [54] (1):

$$k = \frac{I_{\beta 1}}{I_{\beta 1} + I_{\alpha 1} + I_{\alpha 2} + I_{\alpha 3}} \cdot 100\% \quad (1)$$

where,

I —diffraction intensity by following crystallographic planes:

$I_{\beta 1}$ —(300) β phase,

$I_{\alpha 1}$ —(110) α phase,

$I_{\alpha 2}$ —(040) α phase,

$I_{\alpha 3}$ —(130) α phase.

$I(300)$ is the diffraction intensity by Bragg diffraction angle $2\theta = 16^\circ$ characteristic for the hexagonal β phase of polypropylene, corresponding to crystallographic plane with Muller indices (300).

2.7. Hardness Test

The hardness of the samples was measured by means of Shore Durometer (Sauter GmbH, Wutöschingen, Germany) where the measurements were performed by a penetration distance of about 5 mm one to each other on the samples surface. The average value of 10 measurements was presented as the result of measurements.

2.8. Tribological Tests

Tribological tests were realized by using the tribological tester BRUKER UMT2 Tribolab (Bruker Corporation, Billerica, MA, USA), operating at the pin-on-flat configuration under reciprocation displacement.

Samples were examined in accordance with the applicable standards (ASTM G99). The pin, a ball made of 1.2378 steel (a diameter of 6.35 mm and a roughness of $R_a = 0.6 \mu\text{m}$) was held in continuous sliding contact with the composite specimen, according to methodology described by Czapczyk et al. [55].

The tribological test with a duration of 60 min and an amplitude 40 mm by maximal velocity 25 mm/s was realized. The tests were carried out for three values of force, respectively, 5 N, 25 N and 45 N. For further experiments, the middle force value was chosen due to the similar values of the coefficient of friction for all three measurements.

Additionally, the measurements with the force of 25 N were most stable. Coefficient of friction was evaluated by expression (2) [56,57]:

$$\mu = (A_r \tau) / W \quad (2)$$

where μ is the friction coefficient, A_r is real contact area, τ is effective shear strength of contacts, and W is the normal load (N).

For testing with this method, the tribotester was equipped with a fixed table, in which the sample is clamped with a vice. It allows an immobilization of the sample and the prevent it from moving in any way, during the measurement.

The measurements of each composite were carried out at least three parallel experiments, to ensure a relevant statistical evaluation. The average value of friction coefficient is presented with corresponding standard deviations. The tests were conducted in dry sliding conditions and at room temperature. Before investigation the samples were cleaned in the deionized water bath for 20 min.

2.9. Surface Morphology and Topography Tests

The deformation of the dynamically charged sliding surface after tribological test was analyzed by means of scanning electron microscopy (SEM) observations, using the FEI Quanta 250 FEG microscope (FEI Company, Hillsboro, OR, USA). The accelerating voltage was 10 kV, images were recorded in the secondary electron mode. The samples were not covered and the measurement was performed in a low vacuum mode (about 70 Pa).

2.10. Confocal Microscopy

Topography measurements were carried out with the Olympus LEXT 4100 laser scanning microscope (Olympus, Hamburg, Germany). The surface of the sample was scanned with laser light (405 nm), which allowed to collect the topography image and measure the roughness of similar-sized areas analyzed always using the same lens/magnification. The Root Mean Square Roughness are presented as a roughness parameter Root mean square height (Sq). This parameter expands the profile (line roughness) parameter Rq three dimensionally. It represents the root mean square for $Z(x, y)$ within the evaluation area (3) [58]:

$$Sq = \sqrt{\frac{1}{A} \iint_A Z^2(x, y) dx dy} \quad (3)$$

3. Results and Discussion

3.1. Spherulitical Morphology

The microscopic observations in polarized light microscopy (POM) were made using Nikon Eclipse E400 microscope equipped with an Opta-Tech digital camera (OPTA-TECH, Warsaw, Poland) for three types of samples, namely neat iPP, iPP with 0.2 wt.% of PACS and iPP with 0.2 wt.% of DMDBS produced by both mold temperature, 20 °C and 70 °C, are presented on Figure 1.

As it follows from the Figure 1, a significant influence of heterogeneous nucleation on iPP morphology is clearly visible. The neat iPP samples are characterized by well-developed spherulites, where only a low influence of the mold temperature, in a form of slightly better developed morphology by higher mold temperature, may be observed. The spherulitical morphology of iPP nucleated with 0.2 wt.% of both NA's, i.e., PACS and DMDBS, is characterized by homogeneous distribution of very small spherulites, even in cylindrical form, an effect in agreement with many publications [41–53]. Once more, by higher mold temperature slightly larger spherulites are developed by cooling induced crystallization.

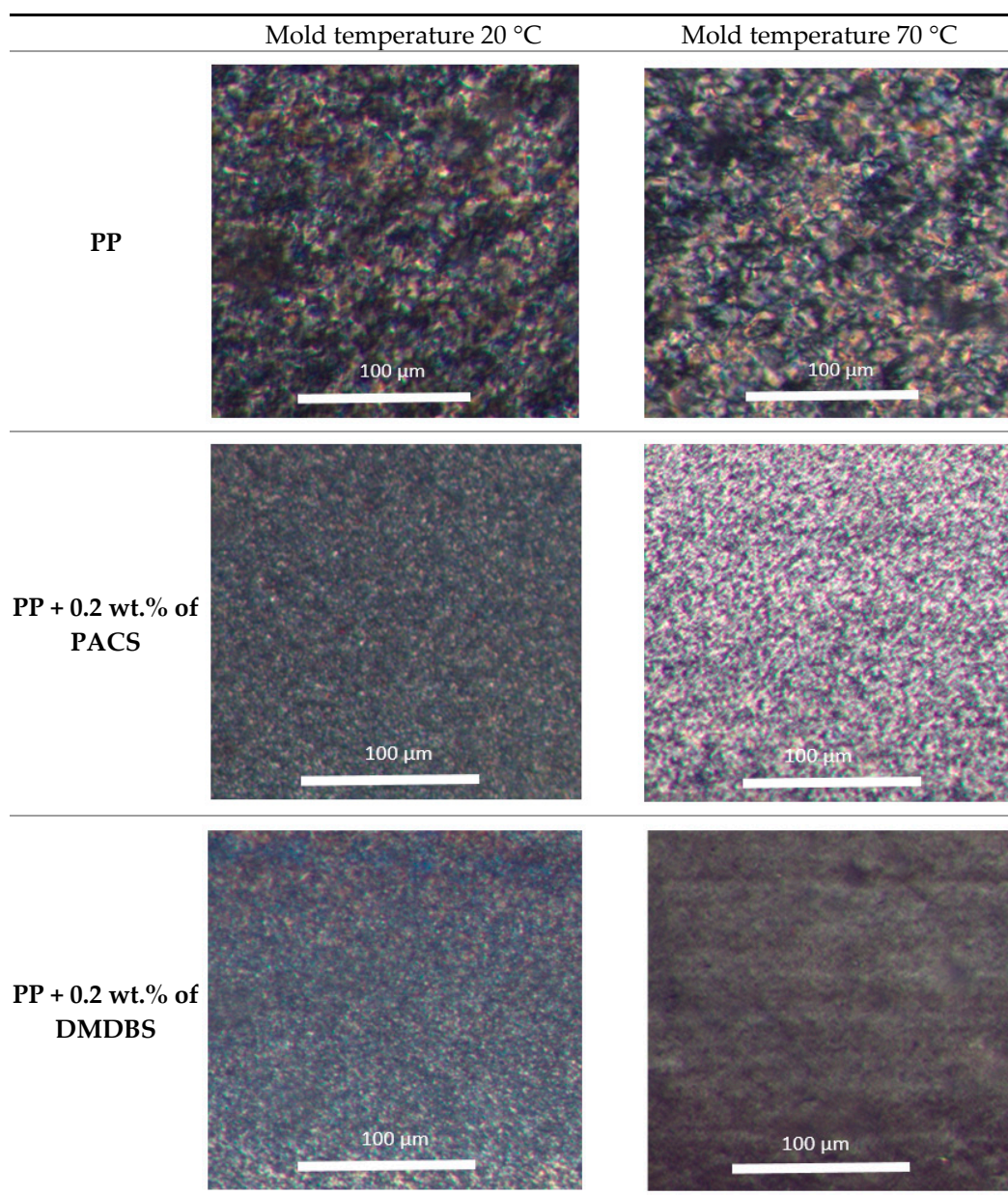


Figure 1. The microscopic observations by polarized light (POM).

3.2. Melting and Crystallization Temperature by DSC

The melting and crystallization temperature of non-modified and modified iPP samples, measured by differential scanning calorimetry, are presented in Table 3.

These results were recorded during second DSC run, as by first heating and cooling not only the structure of investigated polymer, but also its thermal and mechanical history are reflected, such as a specific ordering of the macromolecular network in a form of macromolecular orientation. Thus, for the structure determination more credible is the second run, realized for samples crystallized in protective atmosphere in controlled constant cooling rate. The DSC results, i.e., the melting and crystallization temperature, characteristic for both iPP crystal phases, measured during second DSC run, are presented in Table 3. As it follows from the Table 3, for samples modified with β -phase NA a characteristic double melting temperature was observed. According to [52] the first peak at the temperature about 151 °C is attributed to melting of the hexagonal— β iPP crystalline phase, followed by iPP recrystallization in monoclinic form, and subsequently melting of the monoclinic—

α -phase of iPP, observed at the temperature at the range of 167 °C. The double melting peaks was not observed in the case of DMDBS and 3 D1 P samples, signifying that in these samples only α -form crystals exist.

Table 3. The melting and crystallization temperature characteristic for both iPP crystal phases.

Samples	Crystallization Temperature T_{kr} [°C]	Melting T_t [°C], First/Second pic (β/α)
PP20	116	148.1/164.1
DMDBS 20	128.4	-/164.8
3 D1 P20	128.4	-/164.6
1 D1 P 20	123.3	150.7/164.5
1 D3 P20	123.7	150.8/167.5
PACS20	123.9	151.0/168.4
PP70	116.3	148.0/163.7
DMDBS70	128.2	-/165.0
3 D1 P70	128.4	-/164.4
1 D1 P70	123.5	150.6/163.1
1 D3 P70	123.5	151.1/167.6
PACS70	123.8	151.0/167.6

By DSC cooling run, a shift of crystallization temperature, depending on the composition of the NA's may be seen. A significantly higher crystallization temperature was observed relatively to the content of the α -monoclinic NA, due to superior nucleation efficiency of this additive [50,51].

3.3. The Polymorphic Crystalline Structure by WAXS

The existence and coexistence of both, monoclinic and hexagonal crystallographic phases was confirmed by Wide-Angle-X ray Scattering (WAXS) measurements, signifying the presence of a polymorphic effect [35,44,59,60] as shown by Garbarczyk and others. The value of k , characteristic for pseudo-hexagonal β -phase content, evaluated by using Turner-Jones equation [54], for samples modified with DMDBS and PACS, are presented on Figure 2. The value of $k = 0$ signifies the existence only of an α monoclinic crystal form, and the $k = 1$ denotes the fully developed β -phase in polypropylene. The k -value ($0 < k < 1$) is a proof of the polymorphism, characteristic for a coexistence of both crystallographic forms. For the neat iPP samples crystallized by mold temperature of 20 °C, as well as for samples containing only the DMDBS and the majority (3:1 DMDBS:PACS) of this NA, only the monoclinic α -phase was detected, an observation concerning both mold temperature, i.e., 20 °C and 70 °C. For other samples an increase of the k -value (β -phase contain) is related with growing concentration of PACS nucleating agent. A certain k -value observed in the case of neat iPP crystallized by injection mold temperature of 70 °C may be explained by effect proposed by Varga [52,53]; a possibility of β - phase creation by high shearing in molten state, what is the case of injection molding. This effect may be observed by relatively high mold temperature, where a lower cooling rate, let to create this crystalline structure at the temperature above the $T_{\alpha/\beta}$ transition state.

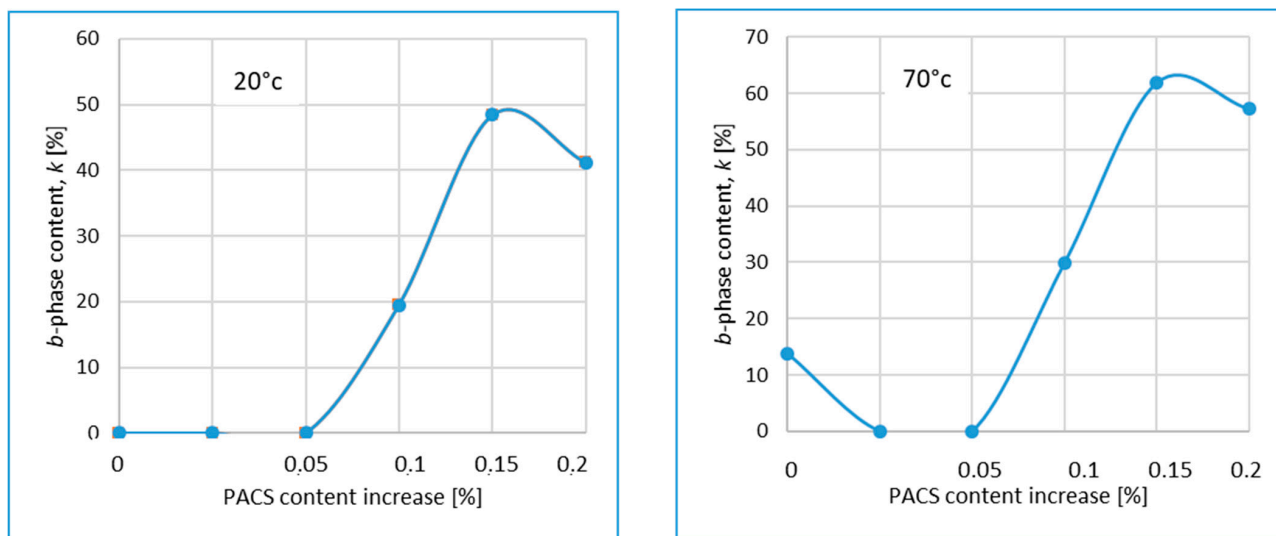


Figure 2. The value of k for samples modified with DMDBS and PACS for 20 °C and 70 °C.

3.4. Hardness Measurements

The hardness values of investigated samples are presented in Figure 3. An increase of the Shore values, depending on the DMDBS content is clearly noticeable, particularly in the case of higher mold temperature. This tendency was observed for all samples, with an exclusion of iPP modified entirely with PACS, where the hardness values are lower and seems to be less mold temperature dependent.

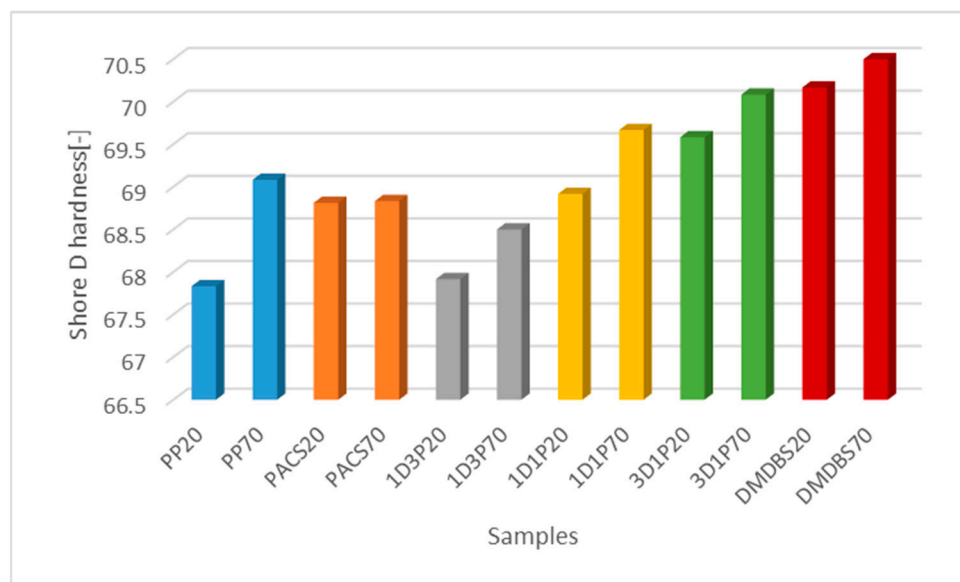


Figure 3. The Shore D hardness of the PP samples with various NA's composition produced by mold temperature of 20 °C and 70 °C.

Another observation was a slight decrease of hardness, for very low DMDBS content (Figure 4) with simultaneous increase of the relative content of β -form NA, (comp. Table 1) responsible for the creation of iPP with lower hardness and modulus as well as improved deformability. On the contrary for higher DMDBS concentration an increase of the Shore hardness values was noted. These effects are in agreement with general assumptions that for the α -phase polypropylene, superior modulus and hardness values are usually

observed, as it was also shown by Aboulfaraj et al. [61] in relation to specific design of lamellas of α and β spherulites.

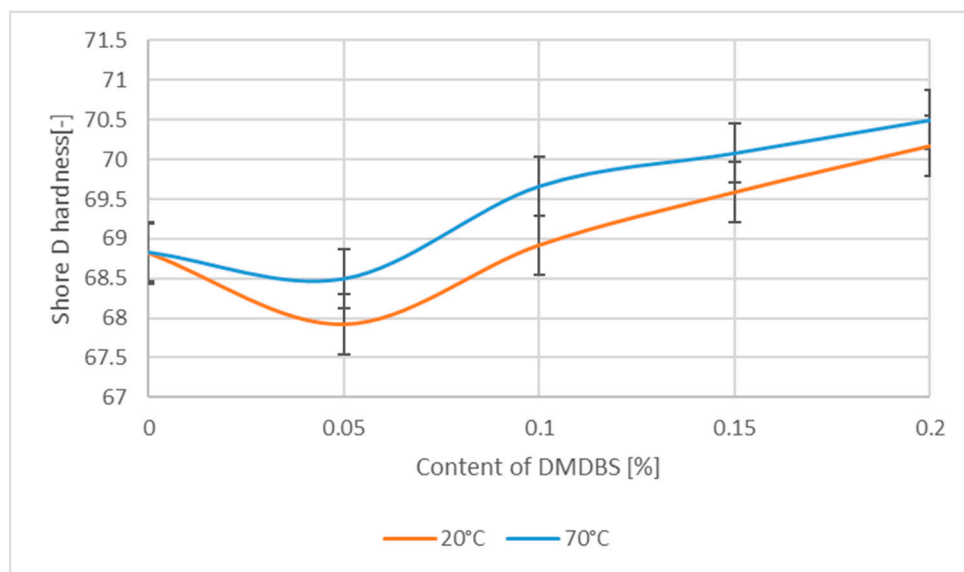


Figure 4. The Shore D hardness as a function of the DMDBS contain in the PP samples.

3.5. Evaluation of Tribological Properties

The charts of changes in the friction coefficient were obtained automatically from tribological tests using the computer software attached to the BRUKER UMT TriboLab device. For all samples the value of the friction coefficient was stabilized after certain patch way (Figure 5).

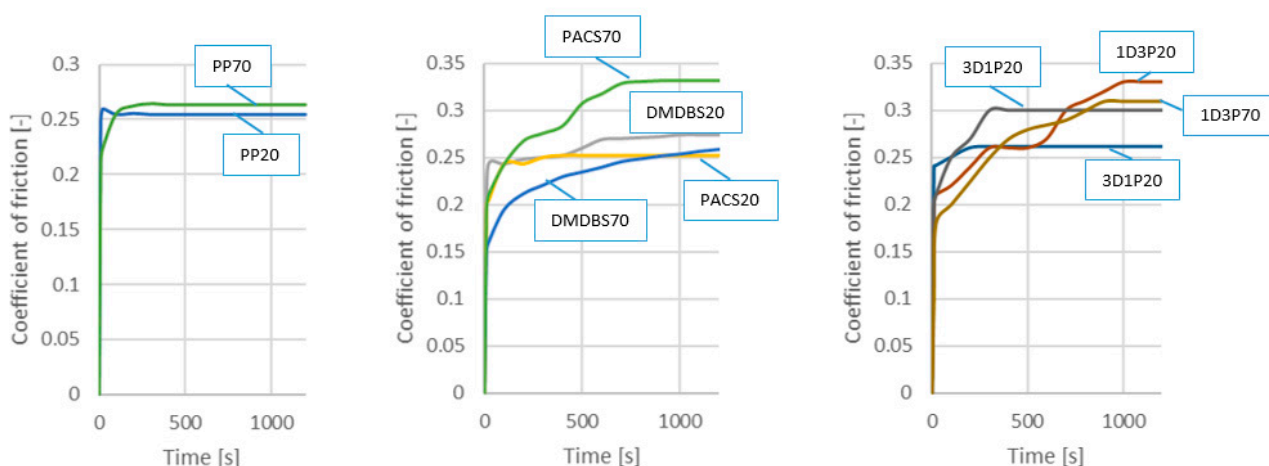


Figure 5. The coefficient of friction as a function of the sliding distance for the samples 20 °C and 70 °C for the normal load of 25 N.

A tendency of sliding distance dependent stabilization of the steady state COF values for PP samples with various NA's composition, produced by mold temperature 20 °C and 70 °C, may be seen on Figure 5.

As it follows from Figure 5, at the beginning of the measurement the coefficient of friction is relatively low and the grows to finally achieve a steady state. This behavior is typical for polymers [62,63]. Due to the adhesion of the polymer to the steel counter-sample, a thin layer of polymer (so-called transfer film) can be deposited on the opposite

sample [64]. All of those factors contribute to the changes of the coefficient of friction in function of sliding distance.

Analyzing the changes of Coefficient of friction for all samples (Figure 5), it can be seen that for the samples produced at lower mold temperature the stabilization occurs after a short time. In the case of higher mold temperature, the values of COF are noticeable higher and the stabilization time is generally longer. The differences in stabilization time may result from changes of the outer layer properties, such as more intense friction induced deformation of the surface, as it will be shown later by discussion of confocal observation of the patch tracks.

Additionally, when analyzing the course of individual measurements (Figure 5), it can be noticed that in the case of iPP samples without NA's, the friction coefficient quickly reached the maximum value, while in the case of other materials this process was extended.

The selected values of the friction coefficient, as examples of measurements by different forces are shown in Figure 6. For samples produced by mold temperature of 20 °C the COF reveals generally lower values, comparing with higher mold temperature. The COF for these series of samples (formed by 20 °C mold temperature) reveal values at the range between 0.24 and 0.26, and less influenced by the structure modification. This observation may be explained by an effect proposed by Varga and confirmed by our measurements, i.e., a tendency of α - form crystal structure creation, less dependent on the NA's composition. In the case of higher mold temperature (70 °C) the COF values are in the range between 0.25 and 0.33, i.e., higher and also more differentiated, thus dependent on the crystal structure formed by using of selective α and β NA's.

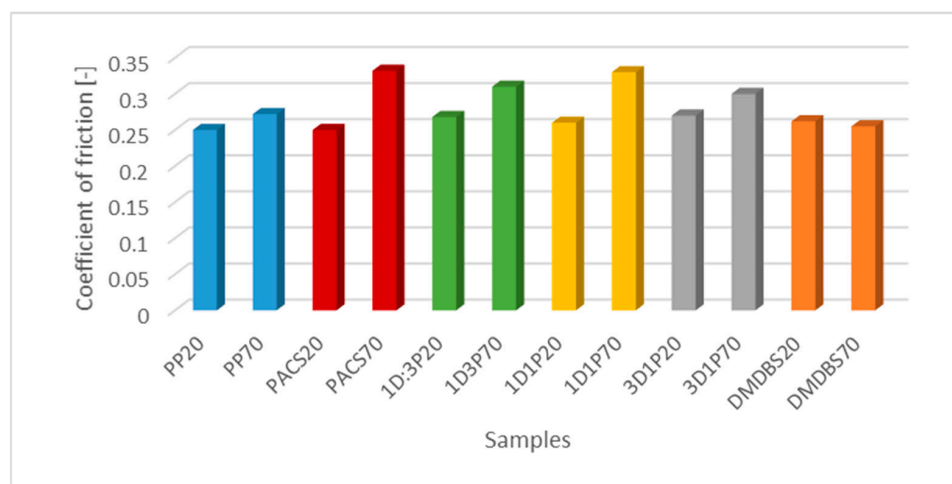


Figure 6. The steady state values of the coefficient of friction of the PP samples with various NA's composition produced by two mold temperature 20 °C and 70 °C.

Analyzing the graph (Figure 7), presenting the value of friction coefficient as a function of the DMBDS, a constant value of COF was observed for a low content of this NA up to 0.1 wt.%. A certain decrease of the COF value of about 40% was noted for the DMBDS content of 0.15 and 0.2 wt.%. These changes are similar for both temperatures.

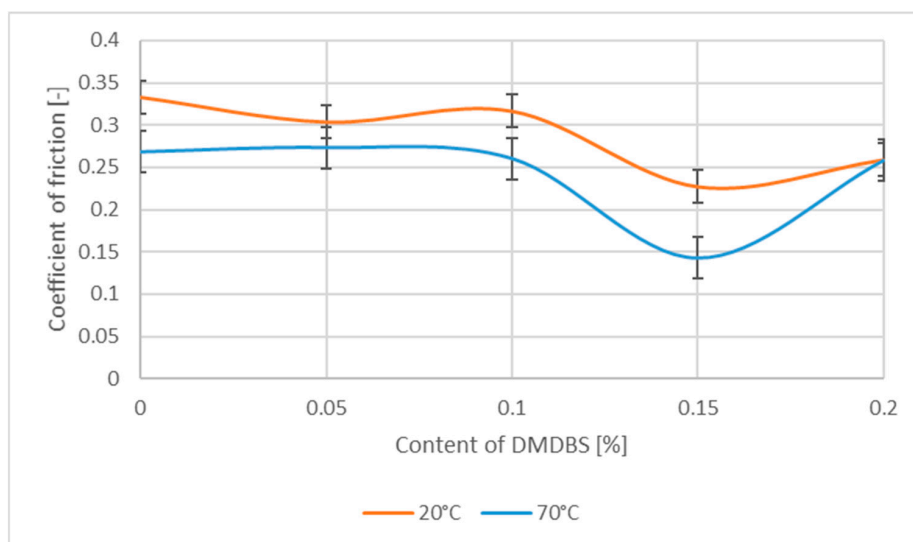


Figure 7. The coefficient of friction as a function of the DMDBS contain in the PP samples.

3.6. Scanning Electron Microscopy and Confocal Microscopy Observation of Friction Area

The friction area was observed by SEM and by confocal microscopy. Furthermore, the roughness after friction test for the sliding patch is presented based on the confocal observations. On the SEM photos a deformational character of the surface of the samples, due to the plastic-like displacement of the skin layer, may be observed. This effect is related to both, the mold temperature by samples production and physical modification of the polymer. Comparing this effect for three types of samples (PP neat polymer, iPP modified with PACS and iPP modified with DMDBS) always a more intense deformation of the samples surface for higher mold temperature was noted. For twin-nucleated samples (formed by 20 °C mold temperature) this effect is also visible, where the intensity of plastic surface deformation is DMDBS content dependent.

The SEM observations are confirmed by results of confocal microscopy, where in addition to surface observation also data’s concerning the vertical displacement of the material were registered. These friction-induced vertical displacements of iPP are shown in a form of 3 D graphs on Table 4, and in numerical values of roughness Sq of the surface before the tests (1) and as scratch formed during the friction test, in Table 5. The width of the friction way observed by confocal microscopy, is presented graphically in comparison with hardness measurements on Figure 8.

Table 4. Comparison of friction area observed by Scanning Electron Microscopy and confocal microscopy.

Samples	Scanning Electron Microscopy	Confocal Microscopy
PP20		

Table 4. Cont.

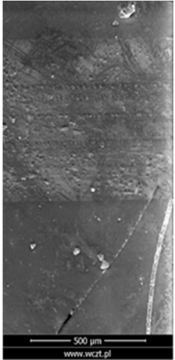
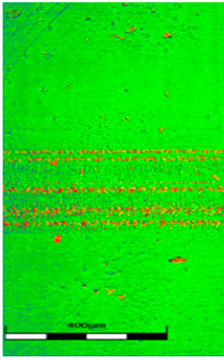
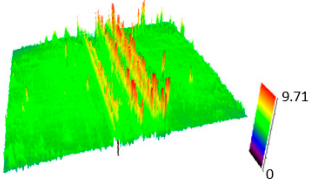
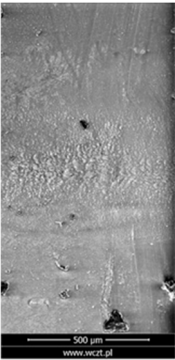
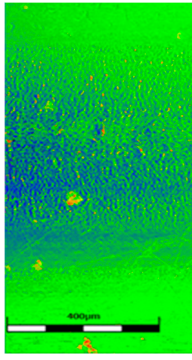
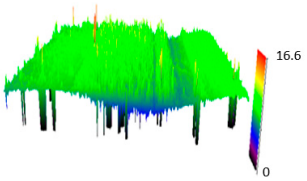
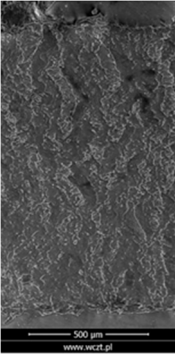
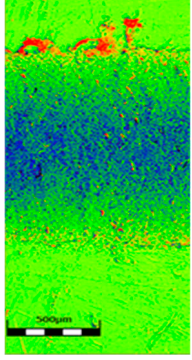
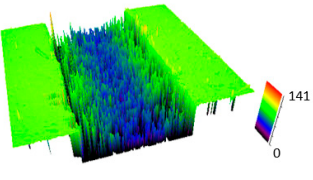
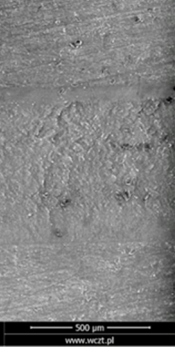
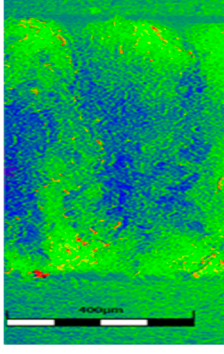
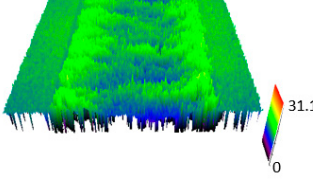
PP70	 <p>SEM image of PP70 surface showing a relatively smooth texture with some fine scratches. Scale bar: 500 µm.</p>	 <p>AFM image of PP70 surface showing a relatively flat topography with some small features. Scale bar: 400 µm.</p>	 <p>3D AFM topography of PP70 surface showing a relatively flat surface with a maximum height of 9.71 nm. Color scale: 0 to 9.71 nm.</p>
PP + PACS20	 <p>SEM image of PP + PACS20 surface showing a more textured surface with some larger features. Scale bar: 500 µm.</p>	 <p>AFM image of PP + PACS20 surface showing a more textured surface with some larger features. Scale bar: 400 µm.</p>	 <p>3D AFM topography of PP + PACS20 surface showing a more textured surface with a maximum height of 16.6 nm. Color scale: 0 to 16.6 nm.</p>
PP + PACS70	 <p>SEM image of PP + PACS70 surface showing a highly textured surface with many small features. Scale bar: 500 µm.</p>	 <p>AFM image of PP + PACS70 surface showing a highly textured surface with many small features. Scale bar: 500 µm.</p>	 <p>3D AFM topography of PP + PACS70 surface showing a highly textured surface with a maximum height of 141 nm. Color scale: 0 to 141 nm.</p>
PP + DMDBS20	 <p>SEM image of PP + DMDBS20 surface showing a highly textured surface with many small features. Scale bar: 500 µm.</p>	 <p>AFM image of PP + DMDBS20 surface showing a highly textured surface with many small features. Scale bar: 400 µm.</p>	 <p>3D AFM topography of PP + DMDBS20 surface showing a highly textured surface with a maximum height of 31.1 nm. Color scale: 0 to 31.1 nm.</p>

Table 4. Cont.

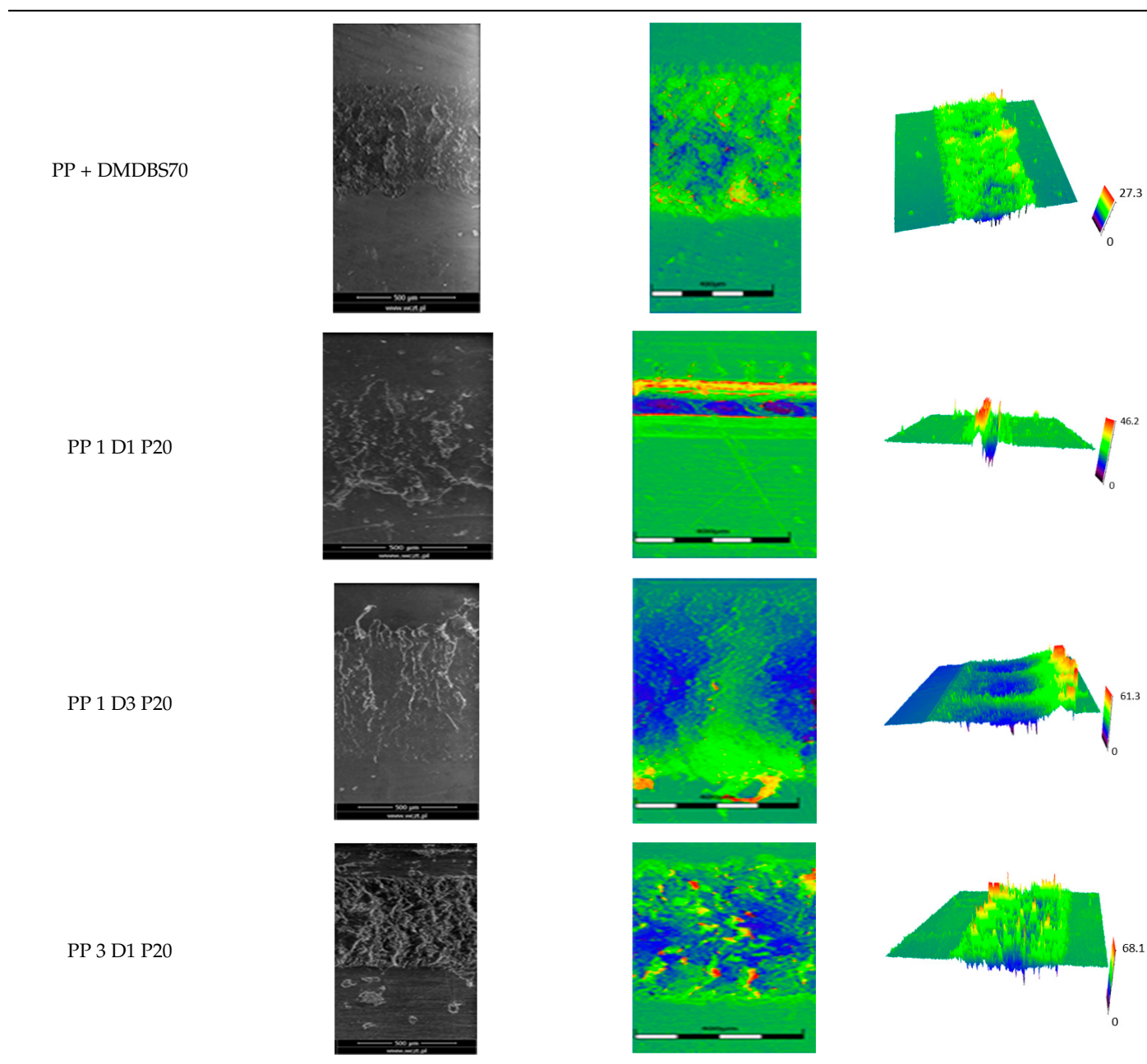


Table 5. The roughness parameter of the surface before the tests (Sq1) and as scratch formed during the friction test (Sq2).

Sample	Sq1 [μm]	Sq2 [μm]	ΔSq
PP20	2.03	1.83	−0.2
PP70	0.54	1.75	1.21
PACS20	0.73	2.18	1.45
PACS70	1.81	5.78	3.97
DMBDS20	1.71	3.64	1.92
DMBDS70	0.53	4.48	3.95
1 D1 P20	0.80	7.19	6.38
1 D3 P20	0.72	5.28	4.56
3 D1 P20	0.80	7.19	6.38

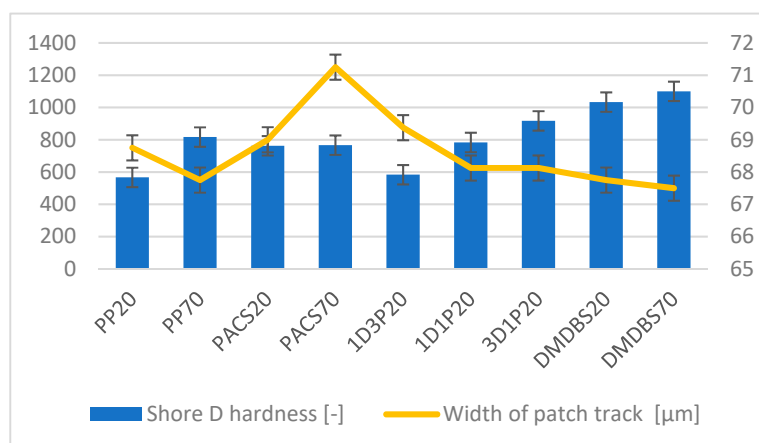


Figure 8. Comparison between hardness of the samples and the width of the patch track.

For all samples, except neat iPP 20, an increase in the roughness value in the area of the scratch, formed after the friction test, compared to the original surface was observed. Two distinct groups of samples were observed: the first one (PP70, PACS20, PACS70, DMBDS20) with a roughness value between 100 and 250%, and the second (DMBDS70, 1D1P20, 1D3P20, 3D1P20) with corresponding roughness between 600 and 800%. These outcomes are in agreement with a former analysis of the SEM observations, where also for the same group of samples more intense displacement of the friction surface was observed. The possible explanation may originate by a higher deformation susceptibility of the surface where the α -modification leads to somehow higher hardness, and consequently to lower relaxation of local pin induced deformation of the surface during the frictional test.

On Figure 8 comparison between hardness of the samples and the width of the patch track, measured by the confocal microscopy, may be seen. As discussed already before, a correlation between the specific nucleation induced structure and the hardness value is observed. The width of the tracks produced by friction test are at the range between 500 and 1200 mm, where the highest values correspond to the hexagonal structure of iPP, i.e., to the polymer with the biggest potential plastic deformability. It may be assumed that these samples, under friction load, undergo a plastic deformation resulting in a superior width and lowest depth of the friction tracks. Consequently, the coefficient of friction of these samples is slightly higher, particularly for the material produced by injection molding with a mold temperature of 70 °C, leading to higher content of the β -phase.

4. Conclusions

The presence of both, monoclinic and hexagonal crystallographic phases was confirmed, signifying the existence of a polymorphic effect. Hardness increases along with DMBDS content where the changes are similar for both mold temperatures. The value of the coefficient of friction depends on the nucleation agent content and the mold temperature. For the 20 °C, lower deformation of the patch track surface occurs and the content of individual additives do not significantly affect its value. However, in the case of 70 °C, these values are higher and more divergent depending on the composition.

The use of 0.15 wt.% of DMBDS, by both mold temperatures, 20 °C and 70 °C, leads to higher resistance of the misshaping of the patch track. This effect is related to both, the mold temperature by samples production and to physical modification of the polymer. Comparing this effect for three types of samples (PP, PACS—modified and DMBDS—modified) always a more intense deformation of the samples surface for higher mold temperature was noted. For twin-nucleated samples (formed by 20 °C mold temperature) this effect is also visible, where the intensity of plastic deformation is slightly DMBDS content dependent.

Based on the mechanical tests and optical observations of the structurally modified iPP frictionally tested, samples following conclusions may be formulated.

1. By selective modification of iPP with gradually varying content of α and β nucleating agents samples with various content of hexagonal β phase may be produced.
2. The specific structure creation in an isotactic polypropylene is followed by changes of the mechanical properties, where usually higher hardness for α -modified samples may be observed.
3. By higher mold temperature, resulting in a lower cooling rate, thus by more nucleation induced structures of iPP, somehow higher values of COF were noted.
4. Regarding the geometrical profile of the patch tracks, as observed by confocal microscopy, the height of friction induced scratches is related to the heterogeneous nucleation modified structure of iPP.
5. The width of the tracks, due to the friction provoked plastic deformation of the modified iPP, appears to be dependent on the heterogeneous nucleation induced structure.

Author Contributions: Conceptualization, N.W. and T.S.; methodology, N.W., M.N., T.S.; validation, N.W.; formal analysis, N.W., T.S., M.N.; investigation, N.W., T.S., M.N.; resources, T.S.; data curation, N.W.; writing—original draft preparation, N.W., T.S., M.N.; writing—review and editing, N.W., T.S.; visualization, N.W.; supervision, N.W.; project administration, N.W.; funding acquisition, N.W., T.S., M.N. All authors have read and agreed to the published version of the manuscript.

Funding: This research received no external funding. This work was supported by the Ministry of Science and Education in Poland under Project No. 0614/SBAD/1547 and No. 0512/SBAD/2120.

Informed Consent Statement: Informed consent was obtained from all subjects involved in the study.

Data Availability Statement: Data sharing not applicable.

Acknowledgments: The authors want to thank Jakub Gałka for the preparation of samples and the DSC measurements and to Katarzyna Skórczewska for the WAXS experiments.

Conflicts of Interest: The authors declare no conflict of interest.

References

1. Theiler, G.; Gradt, T. Influence of counterface and environment on the tribological behaviour of polymer materials. *Polym. Test.* **2021**, *93*, 106912. [[CrossRef](#)]
2. Walczak, M.; Caban, J. Tribological characteristics of polymer materials used for slide bearings. *Open Eng.* **2021**, *11*, 624–629. [[CrossRef](#)]
3. Dong, Z.; Chen, B.; Zhang, M.; Li, J.; Wang, S. One-step preparation of carbon fiber-ZrO₂ hybrid and its enhancement on the wear-resistant properties of polyimide. *Polym. Compos.* **2021**, *42*, 2598–2607. [[CrossRef](#)]
4. Hu, C.; Qi, H.; Yu, J.; Zhang, G.; Zhang, Y.; He, H. Significant improvement on tribological performance of polyimide composites by tuning the tribofilm nanostructures. *J. Mater. Process. Technol.* **2020**, *281*, 116602. [[CrossRef](#)]
5. Wu, Y.; Dong, C.; Yuan, C.; Bai, X.; Zhang, L.; Tian, Y. MWCNTs filled high-density polyethylene composites to improve tribological performance. *Wear* **2021**, *477*, 203776. [[CrossRef](#)]
6. Baduruthamal, Z.A.; Mohammed, A.S.; Madhan Kumar, A.; Hussein, M.A.; Al-Aqeeli, N. Tribological and electrochemical characterization of UHMWPE hybrid nanocomposite coating for biomedical applications. *Materials* **2019**, *12*, 3665. [[CrossRef](#)]
7. Aliyu, I.K.; Mohammed, A.S.; Al-Qutub, A. Tribological performance of ultra high molecular weight polyethylene nanocomposites reinforced with graphene nanoplatelets. *Polym. Compos.* **2019**, *40*, E1301–E1311. [[CrossRef](#)]
8. Bashandeh, K.; Tsigkis, V.; Lan, P.; Polycarpou, A.A. Extreme environment tribological study of advanced bearing polymers for space applications. *Tribol. Int.* **2021**, *153*, 106634. [[CrossRef](#)]
9. Pelto, J.; Heino, V.; Karttunen, M.; Rytöluoto, I.; Ronkainen, H. Tribological performance of high density polyethylene (HDPE) composites with low nanofiller loading. *Wear* **2020**, *460–461*, 203451. [[CrossRef](#)]
10. Bashandeh, K.; Lan, P.; Polycarpou, A.A. Tribological Performance Improvement of Polyamide against Steel Using Polymer Coating. *Tribol. Trans.* **2019**, *62*, 1051–1062. [[CrossRef](#)]
11. Mahmoud, M.M.; Ali, W.Y. Abrasion resistance of blended polymers filled with metallic powders. *Mat. Wiss. Werkstofftech.* **2017**, *48*, 731–736. [[CrossRef](#)]
12. Mudradi, S. Dry Sliding Wear Behavior of Cast Iron Powder Filled Epoxy Composite. *AIP Conf. Proc.* **2019**, *2080*, 020020.
13. Xiong, X.; Ma, L.; Zhang, Z.; Yang, H. Mechanical, morphology, crystallization and melting behavior of polypropylene composites reinforced by non-metals recycled from waste printed circuit boards. *Plast. Rubber Compos.* **2021**, *50*, 162–171. [[CrossRef](#)]

14. Lin, T.A.; Lin, J.-H.; Bao, L. Polypropylene/thermoplastic polyurethane blends: Mechanical characterizations, recyclability and sustainable development of thermoplastic materials. *J. Mater. Res. Technol.* **2020**, *9*, 5304–5312. [[CrossRef](#)]
15. Hanna, E.G. Recycling of waste mixed plastics blends (PE/PP). *J. Eng. Sci. Technol. Rev.* **2019**, *12*, 87–92. [[CrossRef](#)]
16. Bispo, S.J.L.; Freire Júnior, R.C.S.; Barbosa, J.F.; Silva, C.C.D.; Côuras Ford, E.T.L. Recycling of polypropylene and curaua fiber-based ecocomposites: Effect of reprocessing on mechanical properties. *J. Strain Anal. Eng. Des.* **2021**, *5*, 1–9. [[CrossRef](#)]
17. Luna, C.B.B.; Siqueira, D.D.; Ferreira, E.S.B.; da Silva, W.A.; Nogueira, J.A.S.; Araújo, E.M. From disposal to technological potential: Reuse of polypropylene waste from industrial containers as a polystyrene impact modifier. *Sustainability* **2020**, *12*, 5272. [[CrossRef](#)]
18. Beck, H.N. Heterogeneous nucleating agents for polypropylene crystallization. *J. Appl. Polym. Sci.* **1967**, *11*, 673–685. [[CrossRef](#)]
19. Binsbergen, F.L. Heterogeneous nucleation in the crystallization of polyolefins: Part 1. Chemical and physical nature of nucleating agents. *Polymer* **1970**, *11*, 117–135. [[CrossRef](#)]
20. Binsbergen, F.L. Heterogeneous nucleation in the crystallization of polyolefins. III. Theory and mechanism. *Polymer* **1970**, *11*, 253–267. [[CrossRef](#)]
21. Wittmann, J.C.; Lotz, B. Epitaxial crystallization of polyethylene on organic substrates: A reappraisal of the mode of action of selected nucleating agents. *J. Polym. Sci. Polym. Phys. Ed.* **1981**, *19*, 1837–1851. [[CrossRef](#)]
22. Wittmann, J.C.; Lotz, B. Epitaxial crystallization of polymers on organic and polymeric substrates. *Polym. Sci.* **1990**, *15*, 909–948. [[CrossRef](#)]
23. Lovinger, A.J.; Chua, J.O.; Gryte, C.C. Studies on the α and β forms of isotactic polypropylene by crystallisation in a temperature gradient. *J. Polym. Sci. Polym. Phys. Part B* **1977**, *15*, 641–656. [[CrossRef](#)]
24. Lotz, B. α and β phases of isotactic polypropylene: A case of growth kinetics ‘phase reentrancy’ in polymer crystallization. *Polymer* **1998**, *39*, 4561–4567. [[CrossRef](#)]
25. Horváth, Z.; Menyhárd, A.; Doshev, P.; Gahleitner, M.; Friel, D.; Varga, J.; Pukánszky, B. Improvement of the impact strength of ethylene-propylene random copolymers by nucleation. *J. Appl. Polym. Sci.* **2016**, *133*, 43823. [[CrossRef](#)]
26. Sterzynski, T. Nucleation by Additives in Semi-Crystalline Polymers: Effects on Mechanical Behavior. In *Performance Of Plastics*; Brostow, W., Ed.; Hanser Publishers: Munich, Germany, 2002.
27. Menczel, J.; Varga, J. Influence of nucleating agents on crystallization of polypropylene. *J. Therm. Anal.* **1983**, *28*, 161–174. [[CrossRef](#)]
28. Garbarczyk, J.; Paukszta, D. Influence of additives on the structure and properties of polymers. *Colloid Polym. Sci.* **1985**, *263*, 985–990. [[CrossRef](#)]
29. Garbarczyk, J.; Sterzynski, T.; Paukszta, D. Influence of additives on the structure and properties of polymers. 4. Study of phase transition in isotactic polypropylene by synchrotron radiation. *Polym. Commun.* **1989**, *30*, 153–157.
30. Gahleitner, M.; Grein, C.; Kheirandish, S.; Wolfschwenger, J. Nucleation of Polypropylene Homo- and Copolymers. *Int. Polym. Process.* **2011**, *26*, 2–20. [[CrossRef](#)]
31. Varga, J. β -modification of isotactic polypropylene: Preparation, structure, processing, properties, and application. *J. Macromol. Sci. Part B* **2002**, *41*, 1121–1171. [[CrossRef](#)]
32. Schlarb, A.K.; Suwitaningsih, D.N.; Kopnarski, M.; Niedner-Schatteburg, G. Supermolecular morphology of polypropylene filled with nanosized silica. *J. Appl. Polym. Sci.* **2014**, *131*, 39655. [[CrossRef](#)]
33. Mileva, D.; Androsch, R.; Zhuravlev, E.; Schick, C.; Wunderlich, B. Homogeneous nucleation and mesophase formation in glassy isotactic polypropylene. *Polymer* **2012**, *53*, 277–282. [[CrossRef](#)]
34. Garbarczyk, J.; Paukszta, D. Influence of additives on the structure and properties of polymers: 2. Polymorphic transitions of isotactic polypropylene caused by aminosulphur compounds. *Polymer* **1981**, *22*, 562–564. [[CrossRef](#)]
35. Nowicki, M. Nano mechanical Analysis of Nucleation Modified isotactic Polypropylene. *Macromol. Symp.* **2018**, *378*, 1600175. [[CrossRef](#)]
36. Labour, T.; Ferry, L.; Hajji, P.; Vigier, G. α - and β -crystalline forms of isotactic polypropylene investigated by nanoindentation. *J. Appl. Polym. Sci.* **1999**, *74*, 195–200. [[CrossRef](#)]
37. Tranchida, D.; Kandioller, G.; Schwarz, P.; Schaffer, W.; Gahleitner, M. Novel characterization of the $\beta \rightarrow \alpha$ crystalline phase transition of isotactic polypropylene through high-temperature atomic force microscopy imaging and nanoindentation. *Polym. Cryst.* **2020**, *3*, 610140. [[CrossRef](#)]
38. Sterzynski, T.; Lambla, M.; Crozier, H.; Thomas, M. Structure and properties of nucleated random and block copolymer of propylene. *Adv. Polym. Technol.* **1994**, *13*, 25–36. [[CrossRef](#)]
39. Sowinski, P.; Piorkowska, E.; Boyer SA, E.; Haudin, J.M. High-Pressure Crystallization of iPP Nucleated with 1,3:2,4-bis(3,4-dimethylbenzylidene)sorbitol. *Polymers* **2021**, *13*, 145. [[CrossRef](#)]
40. Sowinski, P.; Piorkowska, E.; Boyer, S.A.E.; Haudin, J.M.; Zapala, K. The role of nucleating agents in high-pressure-induced gamma crystallization in isotactic polypropylene. *Colloid Polym. Sci.* **2015**, *293*, 665–675. [[CrossRef](#)]
41. Caom, Y.; Van Horn, R.M.; Tsai, C.-C.; Graham, M.J.; Jeong, K.; Wang, B.; Auriemma, F.; Rosa, C.; Lotz, B.; Cheng, S.Z.D. Epitaxially Dominated Crystalline Morphologies of the γ -Phase in Isotactic Polypropylene. *Macromolecules* **2009**, *42*, 4758–4768.
42. Campus, A.; Lafin, B.; Sterzynski, T. Structure-Morphology Modification of Cable Insulation Polymers. In *Proceedings of the 1998 IEEE 6th International Conference on Conduction and Breakdown in Solid Dielectrics*, Vasteras, Sweden, 22–25 June 1998; Institute of Electrical and Electronics Engineers: Piscataway, NJ, USA, 1998; pp. 357–360.

43. Romankiewicz, A.; Sterzynski, T.; Brostow, W. Structural characterization of α and β nucleated isotactic polypropylene. *Polym. Int.* **2004**, *53*, 2086–2091. [[CrossRef](#)]
44. Sterzynski, T.; Oeaysed, H. Structure modification of isotactic polypropylene by bi-component nucleating system. *Polym. Eng. Sci.* **2004**, *44*, 352–361. [[CrossRef](#)]
45. Wang, S.-W.; Leng, Y.-T.; Jiang, J.; Zheng, G.-Q.; Li, Q. Competition between α and β Crystallization in Isotactic Polypropylene: Effect of Nucleating Agents Composition. *Int. Polym. Process.* **2015**, *30*, 344–349. [[CrossRef](#)]
46. Tjong, S.C.; Shen, J.S.; Li, R.K.Y. Morphological behaviour and instrumented dart impact properties of β -crystalline-phase polypropylene. *Polymer* **1996**, *37*, 2309–2316. [[CrossRef](#)]
47. Li, J.X.; Wl, C. Conversion of growth and recrystallisation of β -phase in doped iPP. *Polymer* **1999**, *40*, 2085–2088. [[CrossRef](#)]
48. Dou, Q. Effect of the composition ratio of pimelic acid/calcium stearate bicomponent nucleator and crystallisation temperature on the production of β crystal form in isotactic polypropylene. *J. Appl. Polym. Sci.* **2008**, *107*, 958–965. [[CrossRef](#)]
49. Broda, J.; Baczek, M.; Fabia, J.; Binias, D.; Fryczkowski, R. Nucleating agents based on graphene and graphene oxide for crystallization of the β -form of isotactic polypropylene. *J. Mater. Sci.* **2020**, *55*, 1436–1450. [[CrossRef](#)]
50. Sterzynski, T.; Lambla, M.; Georgi, F.; Thomas, M. Studies of the Trans-Quinacridone Nucleation of Poly-(ethylene-b-propylene): Dedicated to the memory of Prof. Morand Lambla. *Int. Polym. Process.* **1997**, *12*, 64–71. [[CrossRef](#)]
51. Thomas, M. Etude de la Nucleation des (Co)Polymers du Propylene. Ph.D. Thesis, Universite Louis Pasteur Strasbourg I, ULP Strasbourg, France, 1993.
52. Varga, J. Crystallisation, Melting and Supermolecular Structure of Isotactic Polypropylene. In *Polypropylene Structure Blends and Composites*; Springer: Dordrecht, The Netherlands, 1995; pp. 56–115.
53. Varga, J. β -Modification of polypropylene and its two-component systems. *J. Therm. Anal.* **1989**, *35*, 1891–1912. [[CrossRef](#)]
54. Turner Jones, A.; Aizlewood, J.M.; Beckett, D.R. Crystalline forms of isotactic polypropylene. *Makromol. Chem.* **1964**, *75*, 134–158. [[CrossRef](#)]
55. Czapczyk, K.; Zawadzki, P.; Wierzbicka, N.; Talar, R. Microstructure and Properties of Electroless Ni-P/Si₃N₄ Nanocomposite Coatings Deposited on the AW-7075 Aluminum Alloy. *Materials* **2021**, *14*, 4487. [[CrossRef](#)]
56. Cho, D.H.; Bhushan, B.; Dyess, J. Mechanisms of static and kinetic friction of polypropylene, polyethylene terephthalate, and high-density polyethylene pairs during sliding. *Tribol. Int.* **2016**, *94*, 164–175. [[CrossRef](#)]
57. Cho, D.H.; Bhushan, B. Nanofriction and nanowear of polypropylene, polyethylene terephthalate, and high-density polyethylene during sliding. *Wear* **2016**, *352–353*, 18–23. [[CrossRef](#)]
58. Whitehouse, D. *Surfaces and their Measurement*, 1st ed.; Butterworth-Heinemann: Oxford, UK, 2004.
59. Garbarczyk, J.; Paukszta, D.; Borysiak, S. Polymorphism of isotactic polypropylene in presence of additives, in blends and in composites. *J. Macromol. Sci. Part B* **2002**, *41*, 4–6. [[CrossRef](#)]
60. Rhoades, M.; Wonderling, N.; Gohn, A.; Williams, J.; Mileva, D.; Gahleitner, M.; Androsch, R. Effect of cooling rate on crystal polymorphism in beta-nucleated isotactic polypropylene as revealed by a combined WAXS/FSC analysis. *Polymer* **2016**, *90*, 67–75. [[CrossRef](#)]
61. Aboulfaraj, M.; G'Sell, C.; Ulrich, B.; Dahoun, A. In situ observation of the plastic deformation of polypropylene spherulites under uniaxial tension and simple shear in the scanning electron microscope. *Polymer* **1995**, *36*, 731–742. [[CrossRef](#)]
62. Ariharan, A.; Maurya, R.; Sharma, R.K.; Sharma, V.K.; Lohia, S.; Balani, K. Damage mechanics of polypropylene-based composites using progressive- and constant-load scratching. *Polym. Compos.* **2020**, *41*, 3830–3841.
63. Savas, S.; Uvez, H. Structure and resultant mechanical and tribological performance of PP/PLA/carbon fiber/ethylene-butyl acrylate composites. *J. Compos. Mater.* **2018**, *53*, 1299–1317. [[CrossRef](#)]
64. Bahadur, S. Development of transfer layers and their role in polymer tribology. *Wear* **2000**, *245*, 92–99. [[CrossRef](#)]